

In the format provided by the authors and unedited.

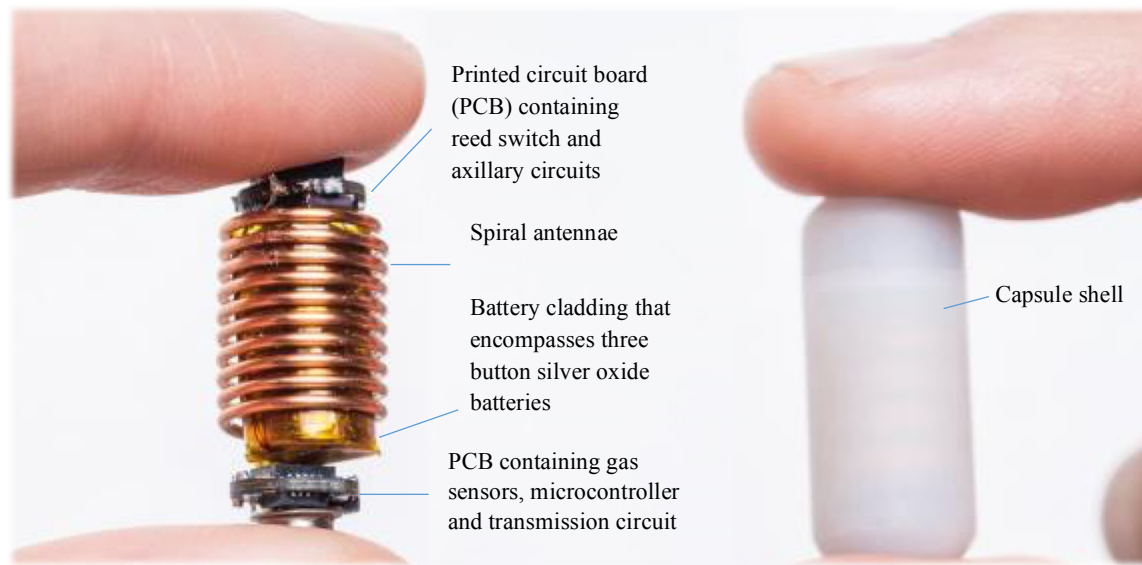
# A human pilot trial of ingestible electronic capsules capable of sensing different gases in the gut

Kourosh Kalantar-Zadeh<sup>1\*</sup>, Kyle J. Berean<sup>1</sup>, Nam Ha<sup>1</sup>, Adam F. Chrimes<sup>1</sup>, Kai Xu<sup>1</sup>, Danilla Grando<sup>2</sup>, Jian Zhen Ou<sup>1</sup>, Naresh Pillai<sup>1</sup>, Jos L. Campbell<sup>2</sup>, Robert Brkljača<sup>2</sup>, Kirstin M. Taylor<sup>3</sup>, Rebecca E. Burgell<sup>3</sup>, Chu K. Yao<sup>3</sup>, Stephanie A. Ward<sup>4</sup>, Chris S. McSweeney<sup>5</sup>, Jane G. Muir<sup>3</sup> and Peter R. Gibson<sup>3\*</sup>

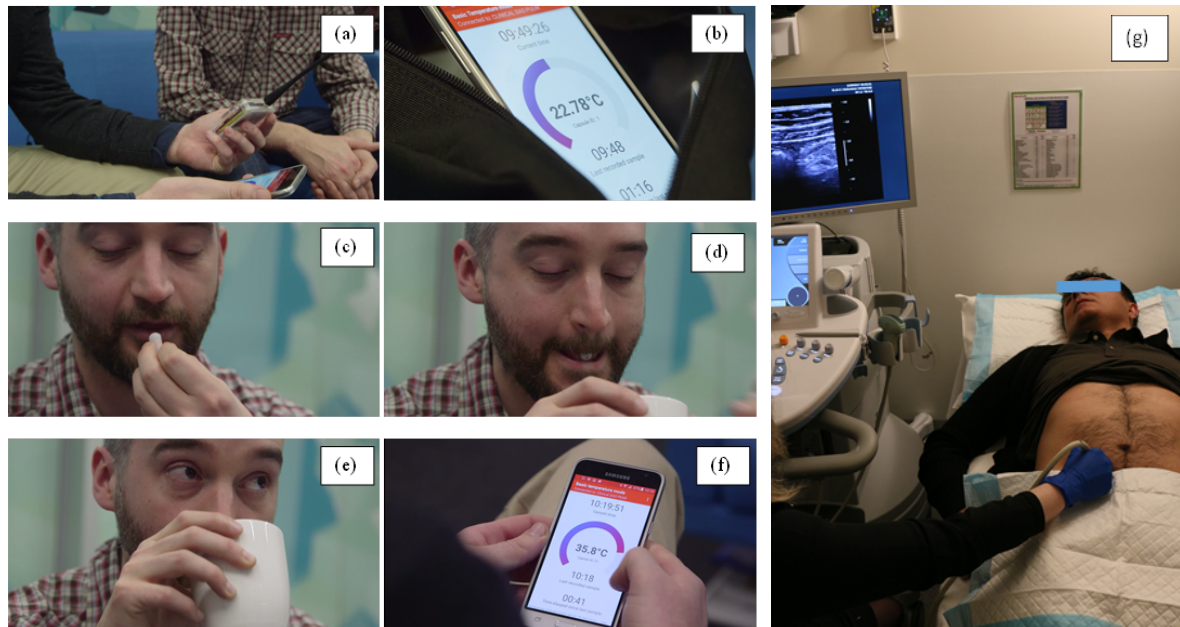
---

<sup>1</sup>School of Engineering, RMIT University, Melbourne, Australia. <sup>2</sup>School of Science, RMIT University, Melbourne, Australia. <sup>3</sup>Department of Gastroenterology, Alfred Hospital, Monash University, Melbourne, Australia. <sup>4</sup>Department of Epidemiology and Preventive Medicine, Monash University, Melbourne, Australia. <sup>5</sup>CSIRO, Agriculture and Food, St Lucia, Brisbane, Australia. \*e-mail: [kourosh.kalantar@rmit.edu.au](mailto:kourosh.kalantar@rmit.edu.au); [peter.gibson@monash.edu](mailto:peter.gibson@monash.edu)

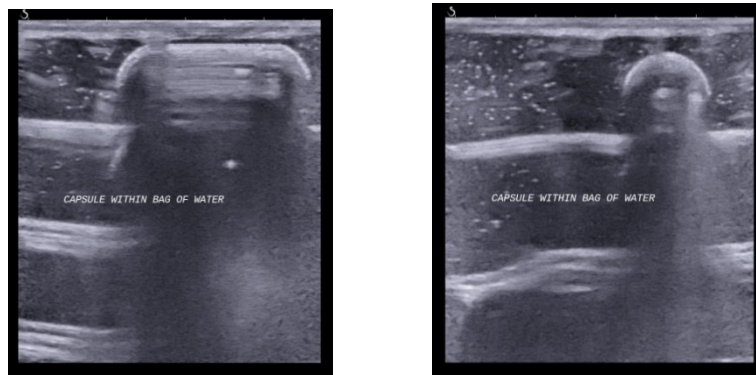
## Supplementary Figures



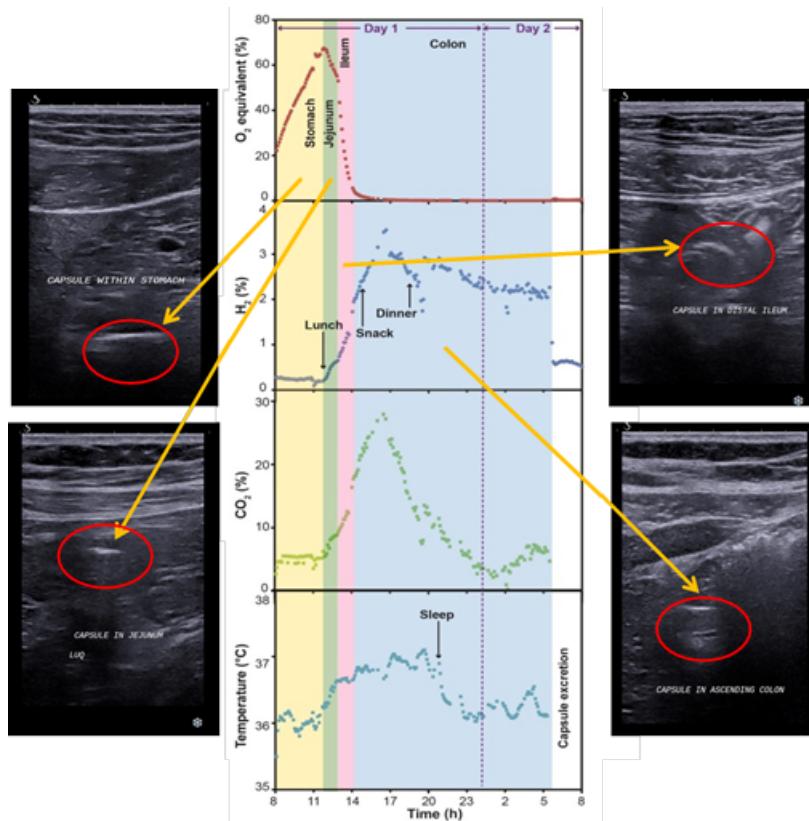
**Supplementary Figure 1** Zoomed in pictures of the inside components of a capsule and its shell



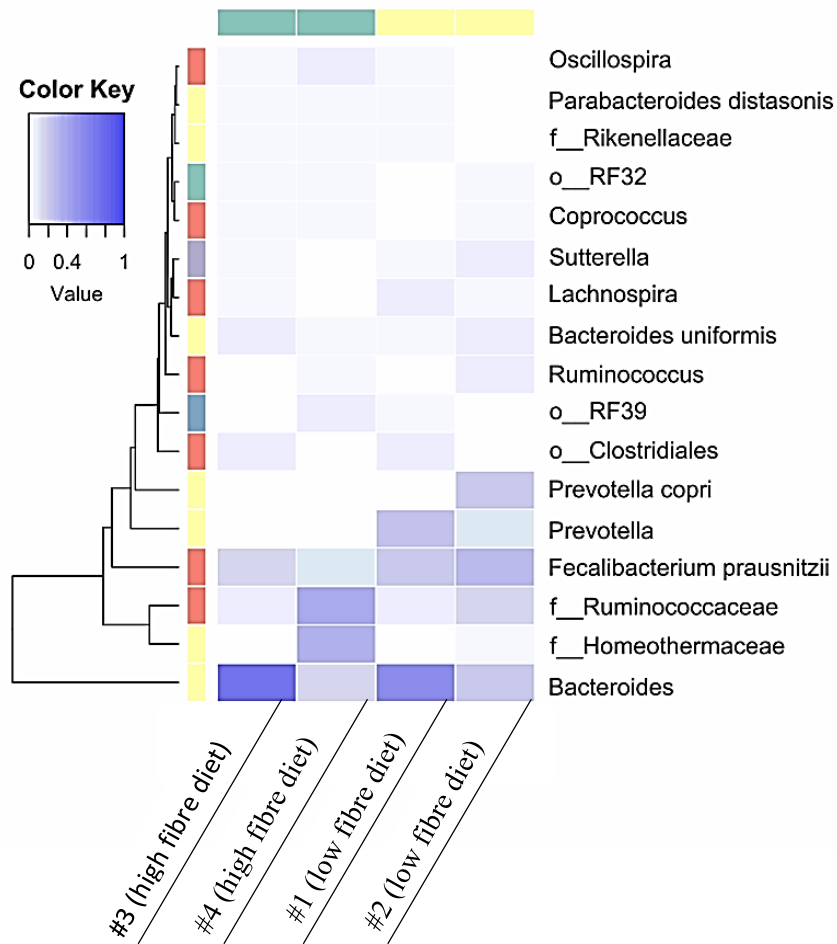
**Supplementary Figure 2** Photographs of a receiver in operation and a volunteer using it. (a) receiver and mobile phone with the operational app. (b) app display showing the capsule at room temperature before being swallowed. (c to e) pictures of a volunteer taking a capsule. (f) the app display shows the core body temperature of the volunteer increased to 35.8°C after capsule was taken and inside the gut. (g) a volunteer during the ultrasound procedure. With written permission from the participants.



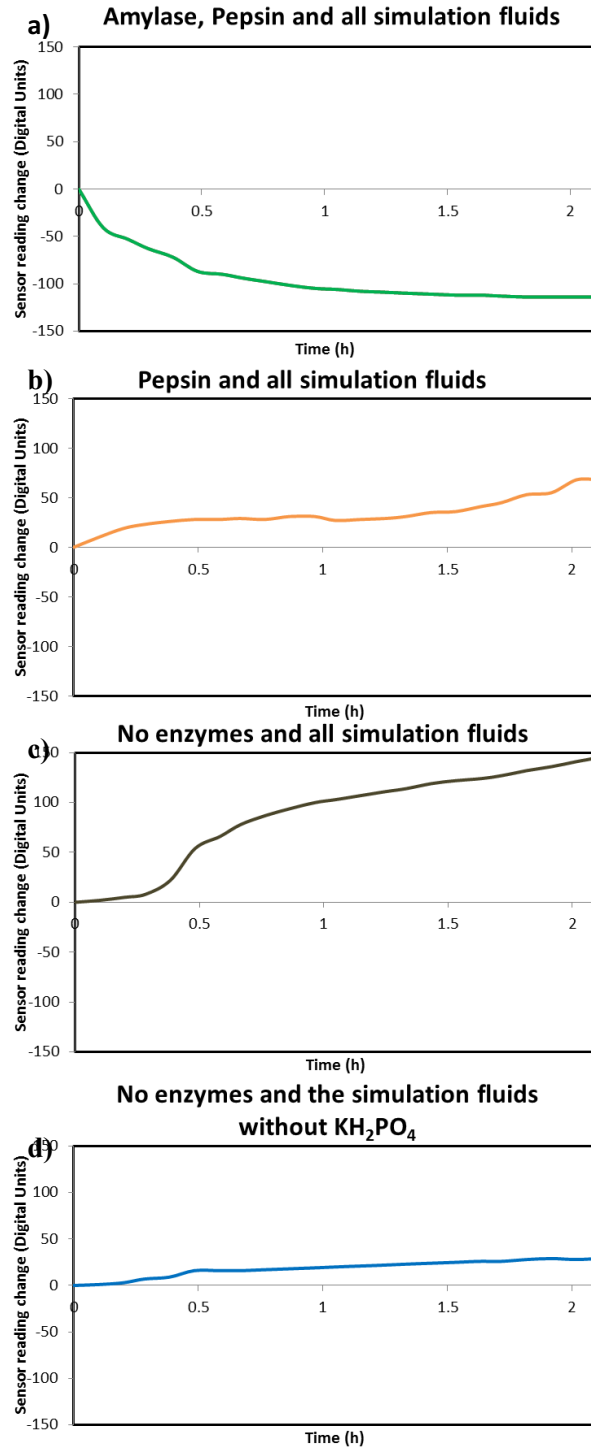
**Supplementary Figure 3** Ultrasound images of the capsule in a bag of water from different angles as a reference.



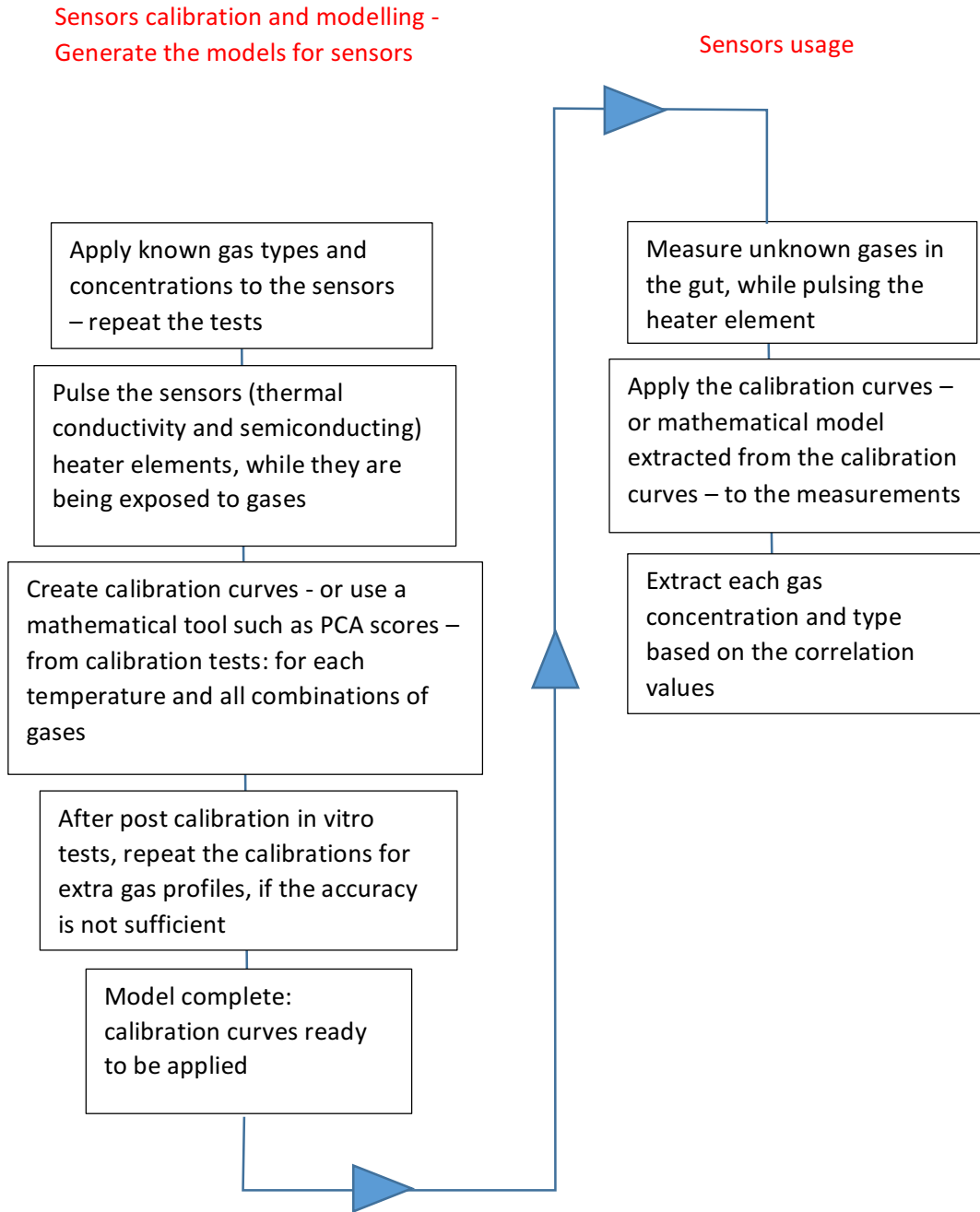
**Supplementary Figure 4** Ultrasound images to associate capsule sensor readings with location in the gut.



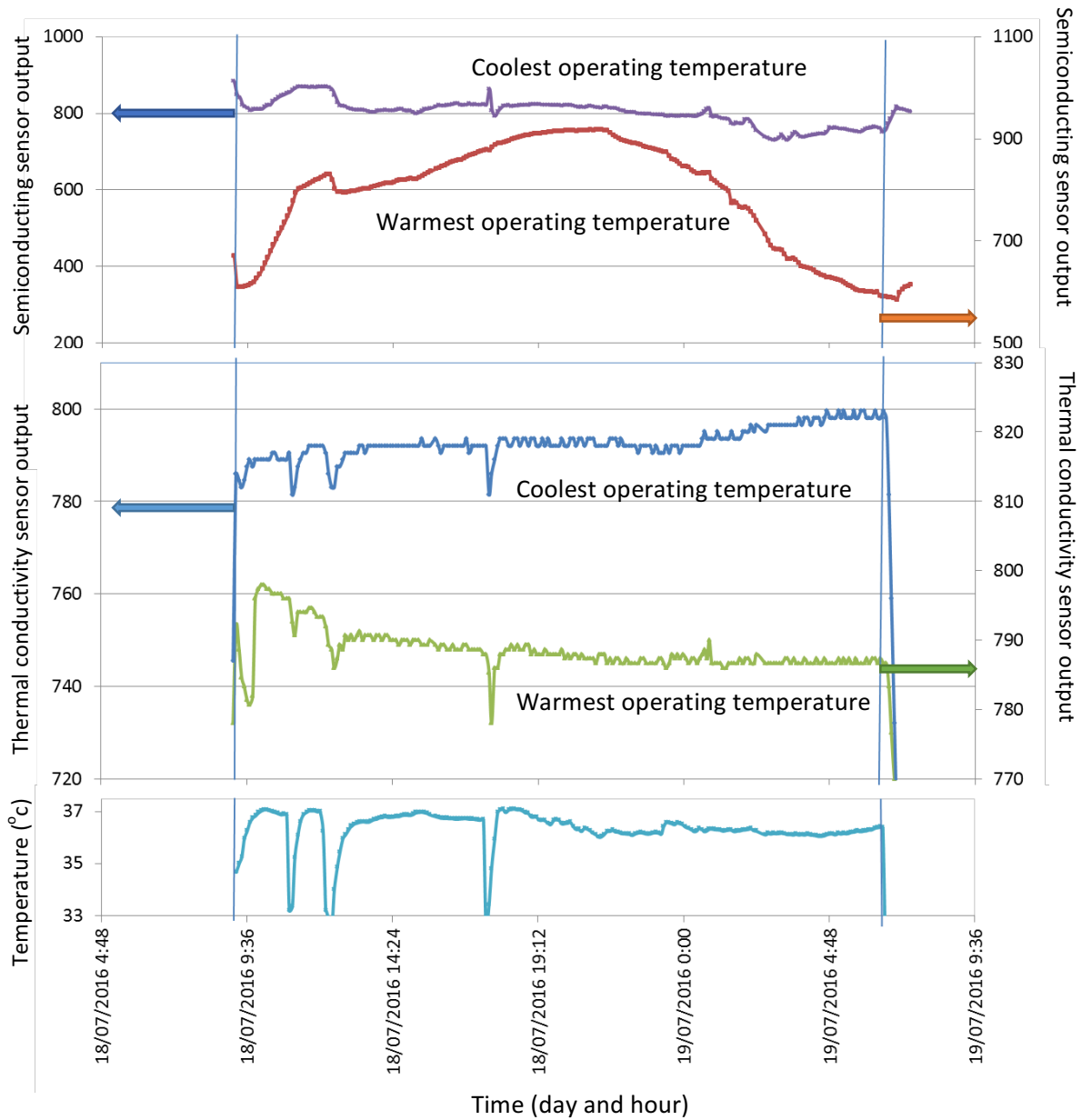
**Supplementary Figure 5** Microbial analysis of repeatability study: Microbial community heatmap - Heatmap of the relative abundance of the community members (operational taxonomic unit; OTU) . Each row represents an OTU clustered at 97% identity. Only OTUs present at  $\geq 5\%$  relative abundance in at least one sample are shown.



**Supplementary Figure 6** Simulations of the origin of the oxidising response to the  $\text{O}_2$  sensor. (a) Oral and gastric phase run with all enzymes and simulated fluids. (b) Oral phase run without amylase but simulated oral fluid and gastric phase run with pepsin and simulated fluid. (c) Oral and gastric phase run with no enzymes and all simulated fluids. (d) Oral and gastric phase run with no enzymes and the gastric simulated fluid has  $\text{KH}_2\text{PO}_4$  removed.



**Supplementary Figure 7** Flow diagram of the extraction algorithm, showing the computational process.



**Supplementary Figure 8** Raw data from **Fig. 3a** from the semiconducting (top), thermal conductivity (middle) and temperature (bottom) sensors before being applied into the extraction algorithm. Only two graphs are presented for thermal conductivity and semiconducting sensors (near the gut temperature and when the sensor heating element is at its warmest point of operation) for clarity of the figures.

## Supplementary Tables

**Supplementary Table 1** Calculated nutritional values for the diet in the ultrasound study

	Energy (MJ)	Protein (g)	Total fat (g)	Carbohydrates (g)	Dietary fibre (g)
High fibre diet (average of all days)	6	66	59	133	33

**Supplementary Table 2** Calculated nutritional values for the diets in the cross over study

	Energy (MJ)	Protein (g)	Total fat (g)	Carbohydrates (g)	Dietary fibre (g)
High fibre diet (average of all days)	8.6	86	105	170	50
Low fibre diet before changing diet to high fibre (average of the first two days)	8.2	113	74	203	15
After shifting from low fibre to high fibre diet (average of the final day)	8.8	89	103	187	44

**Supplementary Table 3** Calculated nutritional values of the diets for the volunteers in repeatability study

	Energy (MJ)	Protein (g)	Total fat (g)	Carbohydrates (g)	Dietary fibre (g)
High fibre - Male	7	69	82	150	36
High fibre - Female	6.5	64	75	141	33
Low fibre - Male	9	85	70	265	23
Low fibre - Female	8.2	82	65	249	22



**Supplementary Table 4** List of chemicals used, concentrations, quantities used, and solution pH. The volumes are calculated for a final volume of 10 mL for SSF, 20 mL for SGF, respectively. The table has been adopted from the work by Minekus *et al.* (4).

Constituent	Stock Concentration		Simulated saliva fluid (SSF)		Simulated gastric fluid (SGF)	
	gL <sup>-1</sup>	ML <sup>-1</sup>	Volume (mL)	pH 7.0 Concentration (mM L <sup>-1</sup> )	Volume (mL)	pH 2.3 Concentration (mM L <sup>-1</sup> )
KCl	37.3	0.5	0.302	15.1	0.276	6.9
KH <sub>2</sub> PO <sub>4</sub>	68	0.5	0.074	3.7	0.036	0.9
NaHCO <sub>3</sub>	48	1	0.136	13.6	0.500	25.0
NaCl	117	2	-	-	0.472	47.2
MgCl <sub>2</sub> (H <sub>2</sub> O) <sub>6</sub>	30.5	0.15	0.010	0.15	0.016	0.1
(NH <sub>4</sub> ) <sub>2</sub> CO <sub>3</sub>	48	0.5	0.0012	0.06	0.020	0.5
*CaCl <sub>2</sub> (H <sub>2</sub> O) <sub>2</sub>	44.1	0.3	0.010	1.5	0.0004	0.15
DI water			9.467		18.679	
For pH adjustment of the stock concentration**						
HCl		6	0.018	1.1	0.052	15.6
Addition of Enzymes						
	U mg <sup>-1</sup>		mg	U	mg	U
*Amylase	38000		0.039	1500	-	-
*Pepsin	10000		-	-	8	80000

\* These ingredients were added just before the phase within the simulation and were not frozen.

\*\* pH balancing should be done before the addition of enzymes. Additional HCl can be added to reach the required stock pH.

## Supplementary Notes

### Inclusion and exclusion criteria for volunteers

The inclusion criteria for trial participants are as follows: 1) healthy males and females aged between 18 to 55 years, 2) non pregnant, 3) BMI less than 27, 4) no implantable devices, 5) no history of: gastrointestinal, cardiovascular, kidney/liver, hormone disorders, high blood pressure or abdominal surgery, and, 6) non-smokers or alcoholics. Additionally the volunteers were required to pass a patency test provided and ascribed by Given Imaging Inc. (Duluth, USA) as per protocol for the Agile™ GI patency test. During the experiments, the volunteer was allowed to continue his day-to-day activities under a controlled and supervised environment, but was not allowed to participate in vigorous physical activity.

The specific exclusion criteria are as follows:

- Pregnancy (Applied to women only)
- Overweight (BMI > 27)
- Implantable device such as heart pacemaker
- A history of gastrointestinal disorders or disease
- A history of cardiovascular disease
- A history of kidney/liver/serious infections
- A history of diabetes or other hormone diseases
- A history of abdominal surgery
- A current smoker
- A current alcoholic (more than two units of alcohol per day for men and more than one unit per day for women)

- Currently suffering from a decreased appetite
- Currently suffering from nausea or vomiting
- Currently suffering from abdominal pain
- Currently suffering from light headedness, shakiness or weakness
- Currently suffering from any chronic condition
- Currently suffering from high blood pressure
- Current participation in a clinical trial (Note: If yes, this is only an exclusion if other trial involves taking a drug or another intervention)

## **Supplementary Methods**

### **Faecal analytical methodology**

#### ***Microbial community analysis***

After an initial bead beating step, DNA extraction using the Maxwell® 16 Research Instrument (Promega) was performed according to the manufacturer's protocol with the Maxwell 16 Tissue DNA Kit (Promega). DNA concentration was measured using a Qubit BR Assay Kit (Life Technologies) and adjusted to 0.2 ng/μl. Libraries were prepared using Nextera XT library prep (Illumina) with Nextera XT indexes, as per manufacturer's instructions. Resulting libraries were quantitated on an Agilent TapeStation System. They were pooled and loaded onto 1/100th of a flow cell per sample and sequenced on the NextSeq 500 (Illumina) using a 2×150 bp High Output V2 kit at the Australian Centre for Ecogenomics (ACE).

#### ***Metabolomic analysis***

High resolution proton and TOCSY NMR spectra were recorded on a 500 MHz Agilent DD2 spectrometer equipped with an OneProbe at 25°C. The residual water signal was suppressed using the PRESAT sequence with 4-step purge. The proton spectra were acquired with 1024 scans with a spectral width of 14 ppm (32768 data points). TOCSY spectra were acquired with 4 scans, 256 increments and with a spinlock time of 80 ms. The spectra were referenced to the TSP singlet (referenced to 0.00 ppm). Spectra were analysed using VnmrJ and ACDLabs NMR processing software. Faecal samples which had already been extracted were transferred to a 5 mm NMR tube for analysis. Identification of the SCFAs was achieved by comparison of the proton and TOCSY NMR data to literature values<sup>1-3</sup>.

### **Localisation of the gas capsule using ultrasound**

The characteristic appearance of the capsule was first assessed *ex vivo* using B-mode imaging with a linear 2-10 MHz probe and a high resolution ultrasound system (SuperSonic Imagine Aixplorer, M4 Healthcare Pty Ltd, Willoughby, New South Wales, Australia). Ultrasound can be reliably used for recognising smart pill location and motility in the gut<sup>4</sup>. Images presented in **Supplementary Figure 3** were taken in a bag of water as a reference to recognise the capsule in the gut. The images shown in **Supplementary Figure 4** evidenced the passage of the capsule through each region of the gut. The gut organ is differentiated by using a combination of anatomical and visual morphological changes seen in the ultrasound images, including thickness of the gut wall and diameter of the bowel.

### **Normalised abundance of microbial communities in the repeatability test**

No discernible separation between the microbial community of the two cohorts (under the influence of high and low fibre diets) was observed in the repeatability test.

### **Exploration of oxidising response to sensor in gastric phase**

#### ***Observations***

In order to determine the origin of the oxygen sensors apparent increase in the stomach, gastric simulations were carried out with the selective removal of components. Four key constituents were chosen to more simply and separate the effects, biologically active components: amylase and pepsin, and ionic components: metal salts and HCl.

It was first demonstrated that when all components were present, a major decrease in the sensor response, indicating the absence of an oxidising agent or a missing O<sub>2</sub> equivalent reading

(**Supplementary Figure 6a**). Indicating that without any food substrates to attach to, the combination of the simulated gut digesta decreases the prevalence of the O<sub>2</sub> equivalent reading. Surprisingly, the removal of amylase changes this dramatically allowing for the rise of the O<sub>2</sub> equivalent reading (**Supplementary Figure 6b**) and furthermore, when pepsin is removed, a significant O<sub>2</sub> equivalent response is seen in the sensor (**Supplementary Figure 6c**).

Given the few salts present in the simulated fluid that could account for this behavior, the simulation was repeated with the removal of the KH<sub>2</sub>PO<sub>4</sub> from the salt and HCl solution. This combination produced no significant increase in dissolved O<sub>2</sub> within the solution, isolating the origin but not the mechanism by which the O<sub>2</sub> profile is produced (**Supplementary Figure 6d**).

The elimination of K<sub>2</sub>HPO<sub>4</sub> from the stomach juice, as the main oxygen source, made the O<sub>2</sub> equivalent profile flat. It was observed that, in the presence of no enzyme, the O<sub>2</sub> equivalent was almost doubled with reference to the baseline value. Interestingly, the addition of pepsin in the full juice in the stomach phase reduced the O<sub>2</sub>-equivalent production with reference to no enzyme case. However, the addition of amylase to the oral phase markedly reduced the O<sub>2</sub>-equivalent concentration. This reduction was in agreement with the drop in the measured O<sub>2</sub> profile in **Supplementary Figure 3a** after the food consumption while the capsule was in the stomach.

### ***Experimental procedure***

Experiments were carried out in a specially designed fermentation vessel fitted with a pressure monitoring system that maintained a constant pressure of 1 Psi throughout the experiment. The capsule was used to monitor the dissolved gas profiles upon sequential removal of components from the simulated oral and gastric fluids. Oral and gastric fluid components were based on Minekus *et al.*<sup>5</sup> (**Supplementary Table 1**). The simulation began with the capsule reaching

equilibrium in air before being placed in 10 ml of DI water within the fermentation vessel which was purged with N<sub>2</sub> for 20 seconds and again allowed to reach equilibrium. The fermentation vessel and all solutions were kept at 37°C prior to addition. Upon equilibration of the capsule within the fermentation vessel, 10 mL of simulated saliva fluid was introduced and allowed 10-15 minutes, or three capsule transmission data points before 20 mL of simulated gastric fluid was added. The solution was then allowed 2 hours at 37°C with gentle shaking before the experiment was complete.

The sequence of experiments were as follows:

1. All components, 10 mL DI water, 10 ml simulated saliva (including amylase), 20 ml simulated gastric fluid (including pepsin).
2. Limited enzymes, 10 mL DI water, 10 ml simulated saliva (minus amylase), 20 ml simulated gastric fluid (including pepsin).
3. Salts only, 10 ml DI water, 10 ml simulated saliva fluid (minus amylase), 20 ml simulated gastric fluid (minus pepsin).
4. Salts minus monopotassium phosphate, 10 ml DI water, 10 ml simulated saliva fluid (minus amylase and KH<sub>2</sub>PO<sub>4</sub>). 20 ml simulated gastric fluid (minus pepsin and KH<sub>2</sub>PO<sub>4</sub>).

### **Extraction algorithm for gas sensors**

Algorithms are briefly described below (based on our two patents: Patent Cooperation Treaty (PCT) application no. PCT/AU2017/000167 and Australian application no. 2017901645):

Semiconducting and thermal conductivity gas sensors were exposed to gas mixtures composed of one or two different gasses from combinations of CO<sub>2</sub>, H<sub>2</sub> and O<sub>2</sub> (in the backgrounds of nitrogen - anaerobic - and ambient air - aerobic). As described in the Methods section, the

extraction algorithm is achieved by analysing the transient responses of the sensors when a pulse is applied to the heater, while the temperature is rising from body temperature to the nominal value operating temperatures of the sensors, within 100 ms. By using the dynamic impedance changes, we were able to provide sensor selectivity using a mathematical algorithm. The establishment of the mathematical algorithm is presented in **Supplementary Figure 7**. Examples of the raw sensor responses from the gut measurements are plotted in **Supplementary Figure 8** (this is for the data of **Figure 3 a**, representing the effect of the high fibre diet in the cross-over study).

The number of calibrations depends on the number of gases to be extracted. In this paper, only CO<sub>2</sub>, H<sub>2</sub> and O<sub>2</sub> were extracted by using ~15 calibration curves with >5 data points each. In this case, high accuracy and good convergence were obtained (data error was within a  $\pm 5\%$  band for each gas profile after the extraction). As the number of calibration curves and points were limited, fitting curves could be manually extracted. However, if more gases and vapours need to be extracted, the number of calibration curves increase resulting in a requirement for computerised machine-learning-based mathematical models such as principal component analysis (PCA). It is important to mention that the thermal conductivity sensor is also ambient temperature sensitive and the effect of drinking cold water is removed by calibrating it against the temperature sensor.



## Supplementary References

- 1 Amiot, A. *et al.* H-1 NMR Spectroscopy of Fecal Extracts Enables Detection of Advanced Colorectal Neoplasia. *J Proteome Re* **14**, 3871-3881, (2015).
- 2 Le Gall, G. *et al.* Metabolomics of Fecal Extracts Detects Altered Metabolic Activity of Gut Microbiota in Ulcerative Colitis and Irritable Bowel Syndrome. *J Proteome Re* **10**, 4208-4218, (2011).
- 3 Wishart, D. S. *et al.* HMDB 3.0-The Human Metabolome Database in 2013. *Nucleic Acids Res* **41**, D801-D807, (2013).
- 4 Kobayashi, Y. *et al.* Sonographic detection of a patency capsule prior to capsule endoscopy: case report. *J Clin Ultrasound* **42**, 554-556, (2014).
- 5 Minekus, M. *et al.* A standardised static in vitro digestion method suitable for food - an international consensus. *Food Funct* **5**, 1113-1124, (2014).